European Journal of Medicinal Chemistry 264 (2024) 115981

Contents lists available at ScienceDirect

European Journal of Medicinal Chemistry

journal homepage: www.elsevier.com/locate/ejmech

Research paper

Synthesis and antimicrobial properties of guanidine-functionalized labdane type diterpenoids

Marina Grinco [a], Olga Moraresc u [a], Francesca Lembo [b], Nicon Ungur [a], Luigia Turco [b], Lorena Coretti [b], Marianna Carbone [c], Carmela Celentano [c,d], Maria Letizia Ciavatta [c], Ernesto Mollo [c], Veaceslav Kulcitki [a,2,**], Elisabetta Buommino [b,1,*]

[a] Institute of Chemistry, State University of Moldova, 3 Academiei str., MD-2028, Chisinau, Republic of Moldova
[b] Department of Pharmacy, University of Naples "Federico II", Via Montesano 49, 80131 Naples, Italy
[c] Consiglio Nazionale delle Ricerche (CNR), Istituto di Chimica Biomolecolare (ICB), Via Campi Flegrei 34, 80078 Pozzuoli Na, Italy
[d] Department of Biology, University of Naples "Federico II", Via Cintia, 21, 80126 Naples, Italy

ARTICLE INFO

Keywords:
Diterpene
Labdane
Acylguanidine
Antimicrobial
Antimicrobial synergism

ABSTRACT

The occurrence of increased antibiotic resistance has reduced the availability of drugs effective in the control of infectious diseases, especially those caused by various combinations of bacteria and/or fungi that are often associated with poorer patient outcomes. In the hunt for novel antibiotics of interest to treat polymicrobial diseases, molecules bearing guanidine moieties have recently come to the fore in designing and optimizing antimicrobial agents. Due to their remarkable antibacterial and antifungal activities, labdane diterpenes are also attracting increasing interest in antimicrobial drug discovery. In this study, six different guanidines prenylated with labdanic fragments were synthesized and evaluated for their antimicrobial properties. Assays were carried out against both non-resistant and antibiotic-resistant bacteria strains, while their possible antifungal activities have been tested on the yeast *Candida albicans*. Two of the synthesized compounds, namely labdan-8,13(*R*)-epoxy-15-oyl guanidine and labdan-8,13(*S*)-epoxy-15-oyl guanidine, were finally selected as the best candidates for further developments in drug discovery, due to their antimicrobial effects on both Gram-negative and Gram-positive bacterial strains, their fungicide action, and their moderate toxicity *in vivo* on zebrafish embryos. The study also provides insights into the structure-activity relationships of the guanidine-functionalized labdane-type diterpenoids.

1. Introduction

Viral, bacterial, and fungal pathogens represent a serious concern in the global context of human health, with a significant impact on the economy worldwide. Indeed, polymicrobial diseases are very difficult to control owing to both their chronicity and the emergence of antibiotic resistance [1–3]. For example, the widespread use of antibacterial drugs is increasingly contributing to the high incidence of pulmonary fungal and bacterial co-infections [4]. Actually, antibiotics are generally developed and tested against single pathogens in isolation, while a therapy based on combined antibacterial and antifungal agents produces important side effects and a strong impact on the non-pathogenic microbiota [5]. In this context, the discovery of novel therapeutic agents able to fight microbes from different families could provide a promising option for addressing modern infectious diseases. In particular, guanidine-containing compounds are emerging as promising antimicrobials that are active against different bacteria and yeasts [6]. The polar nature of the guanidinium functional group represents an important tool for the interaction with the microbial targets *via* a biofilm inhibition and dispersal mechanism which has been demonstrated to be efficient in drug combination therapy [7]. As an example, isopropoxybenzene guanidine exerts a relevant synergistic action in combination with colistin by triggering cytoplasmic membrane damage on binding to phosphatidylglycerol and cardiolipin, leading to the dissipation of proton motive force and accumulation of intracellular ATP [8].

* Corresponding author
** Corresponding author.
E-mail addresses: veaceslav.kulcitki@usm.md (V. Kulcitki), elisabetta.buommino@unina.it (E. Buommino).
[1] Elisabetta Buommino represents the corresponding author for biologic assays.
[2] Vaceslav Kulcitki represents the corresponding author for chemistry troubles.

https://doi.org/10.1016/j.ejmech.2023.115981
Received 2 October 2023; Received in revised form 17 November 2023; Accepted 19 November 2023
Available online 4 December 2023

Abbreviations

AMB	Amphotericin B
ATP	Adenosine Triphosphate
ARB	Antibiotic resistance breakers
CDI	Carbonyldiimidazole
COSY	Correlation spectroscopy
DEPT	Distortionless enhancement by polarization transfer
DMF	Dimethylformamide
DMSO	Dimethylsulfoxide
DNA	Deoxyribonucleic acid
GC	Gas chromatography
GEN	Gentamycin
HMBC	Heteronuclear multiple bond correlation
hpf	Hours post fertilization
HSQC	Heteronuclear single quantum coherence
HWE	Horner-Wadsworth-Emmons
IPM	Imipenem
IR	Infrared spectroscopy
FIC	Fractional inhibitory concentration
Me	Methyl
MIC	Minimal inhibitory concentration
m.p.	Melting point
MRSA	Methicillin-resistant *Staphylococcus aureus*
NMR	Nuclear magnetic resonance spectroscopy
NOESY	Nuclear Overhauser effect spectroscopy
OXA	Oxacillin
Ph	Phenyl
p.p.m.	Parts per million
SAR	Structure-activity relationship
SM	Supplementary material
SP	Staurosporine
t-Bu	*tert*-Butyl
THP	Tetrahydrofuran
TLC	Thin layer chromatography
TMPA	Trimethylphosphonoacetate
TOB	Tobramycin
VAN	Vancomycin
VRC	Voriconazole

The ability of polyhexamethylene guanidine hydrochloride to disrupt bacterial biofilms *via* the formation of guanidine-mediated DNA complexes was also predicted by molecular docking assays [9].

The guanidine scaffold is present in a huge number of bioactive naturally occurring compounds that includes also less common terpenoid based alkyl- and acylguanidines [10]. Within these, the alkyl derivatives such as galegine and pterogynidine (Fig. 1) have shown promising antimicrobial properties against a variety of clinically relevant methicillin-resistant *S. aureus* strains (SA-1199 B, XU212, and EMRSA-16) [11]. Other alkylguanidines have been also explored recently as antibacterial agents and showed remarkable activities [12–14]. On the other hand, the antimicrobial properties of the acylguanidine terpenes like dotofide and actinofide (Fig. 1), reported to date only from marine source [15–17] is still underexplored even if extremely intriguing. Indeed, the acyl guanidines are regarded as more favorite drug candidates, due to their better bioavailability [18,19]. Based on this and continuing our synthetic studies to modify natural scaffolds as to improve their bioactivity [20], we have setup a synthetic route to obtain acylated guanidine derivatives starting from nature-inspired diterpenic carboxylic acids with labdane skeleton to be screened as antimicrobial agents against human drug resistant pathogenic strains representing a critical threat to human health [21].

2. Results and discussion

2.1. Chemistry

2.1.1. Synthesis of labdanic carboxilic acids

The synthesis of labdanic carboxilic acids which were used for guanidine acylation was performed in short sequences starting from commercially available sclareol (**1**) (Scheme 1A). Oxidative degradation of **1** on potassium permanganate treatment [22] provides an excellent yield of hydroxyketone **2**, which is dehydrated and olefinated with trimethylphosphonoacetate (TMPA) to the mixture of labdanic esters. Their alkaline hydrolysis and chromatographic separation deliver pure acids **3** and **4** [23]. On the other hand, acetylation of **1** to the corresponding diacetate and its ozonolytic cleavage provides the diacetylated carboxylic acid **5** [24].

Preparation of heterocyclic labdanic acids **6** and **7**, which are in fact enantiomers of natural gomeric and epigomeric acids [25,26] can be achieved from manoyl oxides **8**, following a hydroboration-oxidation protocol (Scheme 1B). Although there are many procedures for conversion of commercial **1** to oxides **8** [27] their following transformation requires three additional synthetic steps, which makes the overall procedure towards *ent*-gomeric acids (**6**) and (**7**) lengthy.

A shorter synthetic path was considered *via* the hydroxyketone **2**, which is already involved in the current synthetic scheme and can be a good substrate for a tandem Horner-Wadsworth-Emmons (HWE) olefination and oxa- Michael cyclization. Preliminary screening of ketone **2** olefination with TMPA (Scheme 1C) showed that the product yield and selectivity is quite sensitive to the reaction conditions, providing mixtures of both HWE olefination products, bicyclic methyl esters **9** and **10** and various amount of methyl esters of *ent*-gomeric acids **11** and **12**, formed *via* a sequence of HWE olefination and oxa- Michael intramolecular addition.

Tandem Wittig – oxa- Michael reactions are known in the literature and relate mostly to the carbohydrate chemistry [28] while their application in the field of isoprenoids is poorly explored [29,30]. Our preliminary results on the ketone **2** HWE olefination demonstrated that it is a suitable substrate for such a sequence which provides straightforward access to methyl *ent*-gomeroates. Hypothetically, the initially formed bicyclic esters **9** and **10** can cyclize under HWE olefination conditions according to the oxa- Michael pathway and deliver methyl *ent*-gomeroates (**11**) and (**12**). The deprotonated phosphonate ester which normally is used in excess for the HWE olefination can be a suitable base to promote the intramolecular oxa- Michael addition. We

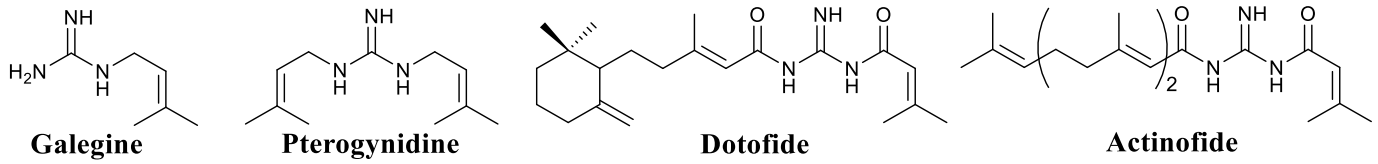

Fig. 1. Natural alkyl and acylguanidines.

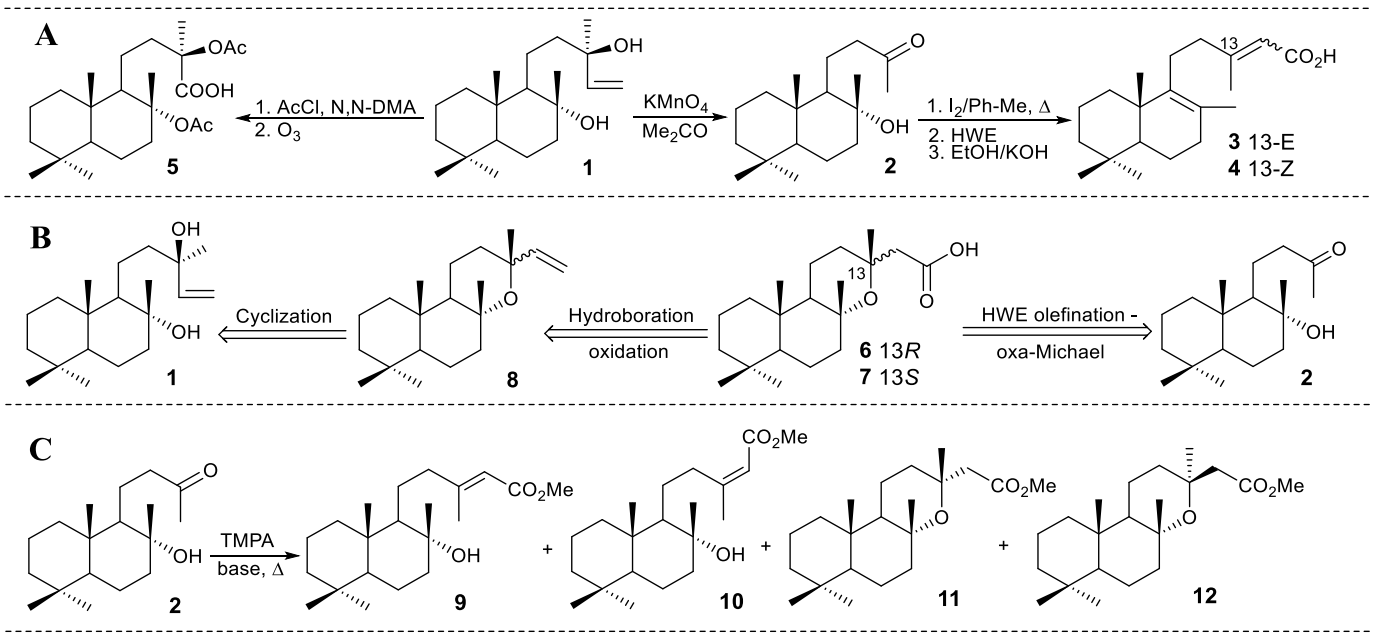

Scheme 1. **A.** Preparation of labdanic acids **3**, **4** and **5**. **B.** Retrosynthetic scheme for the preparation of *ent*-gomeric acids (**6**) and (**7**). **C.** Tandem HWE-oxa- Michael reaction of hydroxyketone **2**.

concluded that a careful tuning of the reaction conditions in terms of solvent and base selection, reagents ratio and reaction duration, can lead to better yields of esters **11** and **12**. The results of this study are shown in Table S1 (see Supplementary Material).

Initial experiments have been performed with three equivalents of TMPA and 3.5 equivalents of sodium methoxide as base (Table S1, entry 1, SM). After 2 h of reflux in benzene GC analysis of the crude product showed a good conversion of starting ketone and formation of moderate amounts of methyl *ent*-gomeroates (**11**), (**12**), along with prevailing bicyclic esters **9** and **10**. Decreasing the excess of base led to poor conversions and total disappearance of methyl *ent*-gomeroates (**11**), (**12**) (Table S1, entries 2 and 3, SM). The same effect had the use of methanol co-solvent and lower phosphonate excess (Table S1, entries 4 and 5, SM). On the contrary, higher phosphonate excess provided the optimum conversion of the ketone **2** to the bicyclic esters **9** and **10** (Table S1, entry 7, SM). At this point it was clear that a slight base excess is required in order to promote the sequential oxa- Michael addition.

Sodium methoxide in benzene showed superior to other bases. Gratifyingly, the use of a higher boiling toluene as the reaction solvent increased the yield of *ent*-gomeroates **11**, **12** and a longer reaction time ensured optimum conditions for their selective synthesis (Table S1, entries 9 and 10, SM).

Due to the similar chromatographic properties, preparative separation of esters **11** and **12** was not possible on flash chromatography. Therefore, the mixture of **11** and **12** was hydrolyzed on refluxing with a methanolic potassium hydroxide solution, which led to the formation of acids **6** and **7**. This mixture was submitted to column chromatography on silica gel, and individual less polar labdan-8,13(*R*)-epoxy-15-oic (**6**) and more polar labdan-8,13(*S*)-epoxy-15-oic (**7**) acids were isolated. The structure of the two compounds was demonstrated on the basis of spectral data, including 1D (^{1}H, ^{13}C, DEPT-135) and 2D homo- (^{1}H–^{1}H COSY, ^{1}H–^{1}H NOESY) and heteronuclear (^{1}H–^{13}C HSQC and ^{1}H–^{13}C HMBC) correlation experiments.

The IR spectrum of acid **6** exhibited absorption bands at 1708 cm^{-1} and 1078 cm^{-1}, suggesting the presence of carboxy- and epoxy-groups. Analysis of ^{13}C NMR, DEPT, and HSQC data showed the presence of 20 carbon signals: five methyl and two methine carbons, eight methylenic and five quaternary carbons, including a carbonyl group (δ_C 171.4). These data match exactly the carbon skeleton of the assigned structure **6**. The careful examination of 2D NMR confirmed the labdane framework containing the C-8 (δ_C 78.6) – C-13 (δ_C 73.5) heterocyclic ring which formed through a tandem Wittig-oxa-Michael reaction, while no double bond was detected. The relative configuration of acid **6** was deduced from NOESY correlations of its methylated derivate, ester **11**, obtained on the methylation of pure **6** with an ethereal solution of diazomethane. In particular, the configuration of the CH_3-17 methyl group was confirmed by CH_3-17↔CH_3-20↔CH_{ax}-11 correlations and no pair correlations between CH_3-17 and CH_2-14 hydrogens (see supplementary material data, Fig. 1). The β-orientation of the CH_3-16 methyl group was proven by pair correlations between CH_3-16↔H_{ax}-11 (Fig. S15, SM).

The structure of epimeric acid **7** was also determined on the basis of its spectral data which were quite similar to those for the epimer **6**. The main difference resided in the stereochemistry of the lateral chain, which was revealed by a NOESY experiment. The β-orientation of the CH_3-17 methyl group was attested by CH_3-17↔CH_3-20↔H_{ax}-11 and CH_3-17↔CH_2-14 correlations indicating that these hydrogens are on the same side (Fig. S7, SM). The α-orientation of the CH_3-16 methyl group is proven by no pair correlations between H_{ax}-11 and CH_3-16 hydrogens demonstrating that the methyl group C-16 is on the opposite molecule face to the methyl at C-17.

Treatment of acid **7** with diazomethane afforded its methylated derivative **12**. According to spectral data, the main signals of the ^{1}H and ^{13}C spectra of ester **12** exhibited a similarity to those of **7**, except for the methyl groups at C-16 and C-17 that appeared as a broad singlet in ^{1}H NMR (see experimental section). The relative configuration of compound **12** was deduced from NOESY correlations of its acid **7**. Thus, having established the structures of acids **6** and **7**, we demonstrated that these compounds are enantiomers of gomeric acids isolated previously from natural sources [25,26].

2.1.2. *Synthesis of prenylated guanidines*

The chemical synthesis of guanidines prenylated with labdanic fragments involved a one-step procedure [31], including the activation of the carboxylic group in acids **3**–**7** with carbonyldiimidazole (CDI), followed by interaction with guanidine base (Scheme 2). The synthesis of bis-acylated guanidine **15** was performed on acylation of guanidine **14** with CDI-activated 3,3-dimethylacrylic acid. All prenylated guanidines have been obtained in good preparative yields (45–52 %) and were

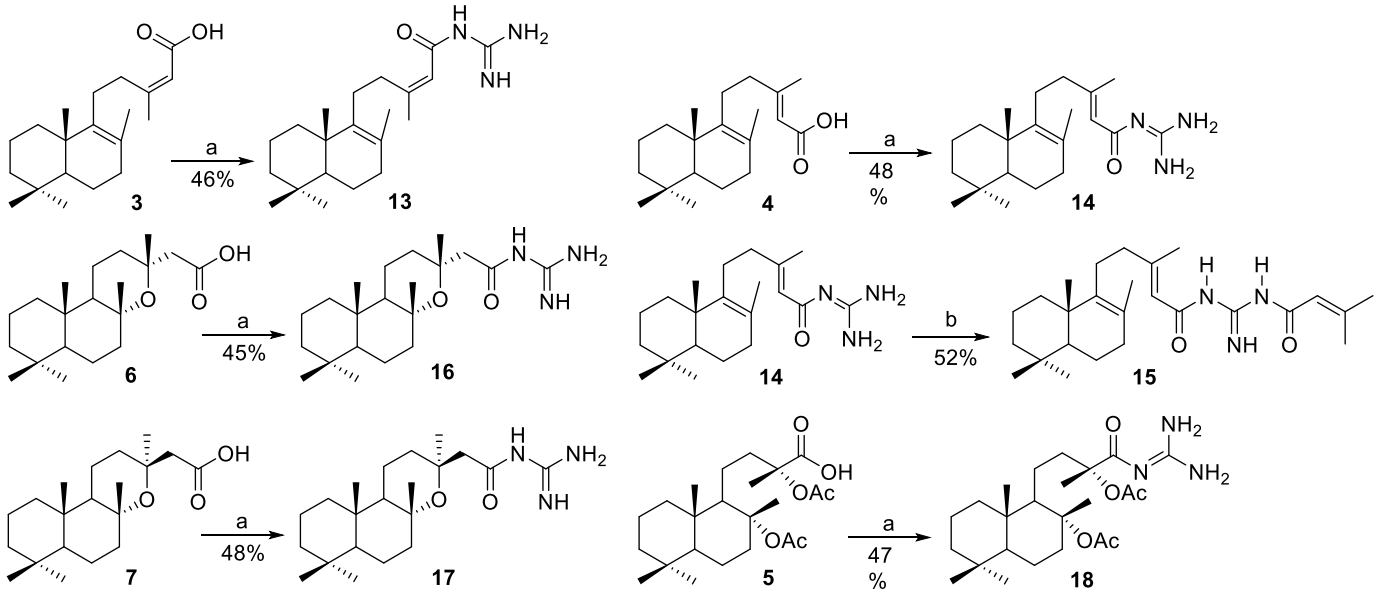

Scheme 2. Reagents and conditions: a) CDI, DMF, then Guanidine-HCl, MeONa, DMF, 3 h; b) 3,3-dimethylacrylic acid, CDI, DMF, then **14**, 3 h.

easily purified by column chromatography on silica gel using methanol-dichloromethane mixtures as eluent.

The structure of prenylated guanidines has been unambiguously demonstrated by spectral analysis. In particular, the infrared spectra show strong absorbance at 3347-3348 cm^{-1} (*N*–H stretching vibration), 1695-1696 cm-1 (C═O), 1584 cm-1 (-NH_2^+ bending vibration), confirming the presence of the acylguanidine fragment. The NMR spectra demonstrate the presence of the tricyclic terpenic heterocycle. Guanidines **16** and **17** are epimeric and differ slightly in both ^{1}H and ^{13}C spectra. Notably, the chemical shifts of angular C-16 and C-17 methyl groups show singlets at 1.34 and 1.26 ppm respectively for **16** and at 1.31 and 1.28 respectively for **17**. The chemical shifts of C-14 methylene groups also differ in both guanidines **16** and **17**, showing doublets at 2.46 and 2.51 ppm respectively for **16** and at 2.69 and 2.74 ppm respectively for **17**. The ^{13}C spectra show differing values for C-8 and C-13 quaternary carbons at 76.1 and 72.8 ppm respectively for **16** and at 76.0 and 72.3 ppm respectively for **17**. The position of carbonyl C-15 carbon is at 173.6 ppm for both **16** and **17**. Elemental analysis confirms the molecular formula for all synthesized acylguanidines.

2.2. Biology

2.2.1. Antimicrobial activity evaluation

Guanidines **13**–**18** were tested for their antimicrobial properties against a series of non-resistant and antibiotic-resistant bacteria strains including *Staphylococcus aureus* ATCC 29213, *S. aureus* ATCC 43300, *S. epidermidis* ATCC 12228, *S. epidermidis* ATCC 35984, *Klebsiella pneumoniae* ATCC 13883, *K. pneumoniae* BAA1705, *Pseudomonas aeruginosa* ATCC 27853, and *P. aeruginosa* PAO1. Except for the diacylated guanidine **15**, which was ineffective or scarcely active, all the synthesized compounds were found to possess antimicrobial activity on all selected strains (see Figs. S3–S7, SM). Compounds **13**, **14**, **16**–**18** were strongly active on Gram-positive strains (Figs. S3 and S4, SM). The MIC values observed ranged between 4 μg/mL and 8 μg/mL, with the best activity observed for guanidine **14** showing a MIC value of 4 μg/mL (Figs. S3–S4) against both *S. aureus* strains, and a MIC of 8 μg/mL against *S. epidermidis* 12228. Guanidine **14** also retained a good activity until 2 μg/mL against the biofilm producer *S. epidermidis* 35984 strain (Fig. S4). Compound **18** totally inhibited the bacteria growth until 16 μg/mL. It is noteworthy that under the same condition oxacillin was not able to contrast the growth of *S. aureus* ATCC 43300 (MRSA) as effectively as guanidines **13**, **14**, and **16**–**18** did.

The antimicrobial effects on the Gram-negative strains were not as strong as on Gram-positive. However, compounds **16** and **17** were active against both *K. pneumoniae* strains, quality control and carbapenem resistant strain, with MIC values of 16 and 32 μg/mL, respectively (Fig. S5, SM). In the same assay, imipenem was not able to contrast the growth of the carbapenem resistant *K. pneumoniae* BAA1705 strain, according to EUCAST 2022 breakpoints [32]. Compounds **16** and **17** also showed a moderate activity at 128 μg/mL against *P. aeruginosa* strains reducing by 70 % and 50 % the growth of *P. aeruginosa* 27853, and by 75 % and by 65 % that of *P. aeruginosa* PAO1, respectively (Fig. S6, SM).

As to investigate their antifungal properties the acylguanidines **13**–**18** were assayed also on the yeast *Candida albicans*. Even in this case, the diacyl derivative **15** was not active. Instead, promising results were observed for the other guanidines getting MIC values of 16 μg/mL for compounds **16, 17** and **18**, and of 8 μg/mL for **13** and **14** (Fig. S7, SM).

The same activity profile was obtained on the azole-resistant *C. albicans* ATCC 10231 strain on which voriconazole was not able to contrast the growth according to CLSI 2022 breakpoints [33]. According to the antimicrobial screening, the attention has been especially focused on the two more promising acyl guanidine derivatives **16** and **17**, that showed antimicrobial properties against Gram-positive, Gram-negative, and the yeast strain. As to gain more information about their mode of action, the minimum bactericidal (MBC) or fungicidal concentration (MFC) of **16** and **17** were investigated and compared with those of their parent *ent*-gomeric acids **6** and **7**. Both acylguanidines resulted bactericidal on *S. aureus*, *S. epidermidis* and *K. pneumoniae*, and fungicide on both strains of *C. albicans*. The MBC was equal to the MIC value reported in Table 1 (MBC results not shown since equivalent to MIC). Conversely, compounds **6** and **7** showed a weaker or null activity on all tested strains (Table 1).

2.2.2. Antimicrobial synergy studies

Considering the activity shown by guanidines **16** and **17** on the drug-resistant strains *S. aureus* ATCC 43300, *K. pneumoniae* BAA1705, and *C. albicans* ATCC 10231, antimicrobial synergy studies were performed by applying the checkerboard method. This technique is used to determine the impact of the combination of antibiotics on their potency in comparison to their individual activities. This comparison is then represented as the Fractional Inhibitory Concentration (FIC) index value, which considers the combination of antibiotics that produces the

Table 1
MIC values against bacterial and yeast strains for guanidines **16** and **17** and parent *ent*-gomeric acids **6** and **7.**

Strains	Compounds MIC, μg/ml										
	16	17	6	7	VAN	OXA	GEN	IPM	TOB	AMB	VRC
S. aureus ATCC 29213	**8**	**8**	**64 (MIC_{70})**	**> 128**	**2**	**2**	ND	ND	ND	ND	ND
S. aureus ATCC 43300	**8**	**4**	**64 (MIC_{70})**	**128**	**2**	**≥ 2 (R)**	ND	ND	ND	ND	ND
S. epidermidis ATCC 12228	**8**	**8**	**64 (MIC_{70})**	**128**	**2**	**2**	ND	ND	ND	ND	ND
S. epidermidis ATCC 35984	**8**	**8**	**64 (MIC_{70})**	**128**	**2**	**2**	ND	ND	ND	ND	ND
K. pneumoniae ATCC 13883	**16**	**16**	**> 128**	**> 128**	ND	ND	**4**	**4**	ND	ND	ND
K. pneumoniae ATCC BAA1705	**32**	**32**	**> 128**	**> 128**	ND	ND	**4**	**≥ 4 (R)**	ND	ND	ND
P. aeruginosa ATCC 27853	**128 (MIC_{70})**	**128 (MIC_{50})**	**> 128**	**> 128**	ND	ND	ND	ND	**2**	ND	ND
P. aeruginosa PAO-1	**128 (MIC_{75})**	**128 (MIC_{65})**	**> 128**	**> 128**	ND	ND	ND	ND	**2**	ND	ND
C. albicans ATCC 90028	**16**	**16**	**> 128**	**> 128**	ND	ND	ND	ND	ND	**4**	**≤ 0,12**
C. albicans ATCC 10231	**16**	**16**	**> 128**	**> 128**	ND	ND	ND	ND	ND	**4**	**≥ 1 (R)**

greatest change from the individual antibiotic's MIC.

Oxacillin was tested in association with guanidines **16** and **17** against *S. aureus* ATCC 43300. After 24 h of incubation we analyzed the results to look for the best combination of **16** and **17** with oxacillin. A complete absence of growth was observed for compound **16** at 4 μg/mL in combination with oxacillin at 0.125 μg/mL, whose MIC is 10 μg/mL on *S. aureus* ATCC 43300. The FICI value of 0.512 was indicative of an additive effect (Table 2). Complete absence of growth was also observed for compound **17** at 2 μg/mL in combination with 0.5 μg/mL oxacillin, with a FICI of 0.550 supporting an additive interaction. Thus, the combination of compounds **16** and **17** with oxacillin slightly increased the inhibitory activity of the guanidines, sustained by the presence of low oxacillin dosage. Similarly, imipenem was tested to look for the best interaction with compounds **16** and **17** against *K. pneumoniae* BAA1705. We observed an additive interaction as well between compounds **16** and **17** at 16 μg/mL in combination with 2 μg/mL imipenem, with a FICI value of 0.600 (Table 2).

Better results were obtained for *C. albicans* ATCC 10231. A growth inhibition was observed for compound **16** at 4 μg/mL in combination with 0.125 μg/mL voriconazole (MIC of voriconazole is 30 μg/mL on *C. albicans* ATCC 10231), with a FICI value of 0.254 indicative of a synergistic interaction (Table 2). A stronger effect and a complete absence of growth was observed for **17** at 2 μg/mL in combination with 0.125 μg/mL voriconazole, with a FICI value of 0.129 supporting a strong synergic interaction. Consequently, guanidines **16** and **17** in combination with voriconazole were able to considerably reduce the concentration of voriconazole necessary to inhibit the growth of the azole resistant strain of *C. albicans* (Table 2).

The combination therapy aims to potentiate the activity of antibiotics [34]. The co-administration of an antibiotic resistance breakers (ARBs) with conventional antibiotics should enhance the effects of the latter combatting the microbial resistance mechanisms, allowing lower doses of drugs to be used (synergic or additive affect). The more successful ARBs achieve greater reductions in the MICs of antibiotics versus antibiotic monotherapy. This is an important aspect in the search of new antimicrobial compounds because reduced antibiotic selection pressure could slow the onset of resistance and reduce the side effects of antibiotic monotherapy. Few data are available to demonstrate the ability of antibacterial compounds bearing prenylated guanidine functional group to act as ARBs in the treatment of microbial infections [6]. The presence of the guanidinium group confers a positive charge to the molecules **16** and **17**. Hypothetically, this may favor the binding of the guanidine derivatives to microbial targets or lead to the disruption of cell membranes and cell wall through electrostatic interaction with the negatively charged bacterial cell envelopes. A similar mechanism might work with the cell wall component of the yeast *C. albicans*.

Table 2
Results of the synergy study for guanidines **16** and **17**/antibiotics combination against the three selected strains. In the table, MIC and FICI values are reported.

Strains	Guanidine 16		Antibiotics		FICI
	MIC alone	MIC in combo.	MIC alone	MIC in combo.	
S. aureus MRSA 43300	8 μg/mL	4 μg/mL	OXA 10 μg/mL	0.125 μg/mL	0.512
K. pneumoniae BAA1705	32 μg/mL	16 μg/mL	IMP 20 μg/mL	2 μg/mL	0.600
C. albicans10231	16 μg/mL	4 μg/mL	VRC 30 μg/mL	0.125 μg/mL	0.254
Strains	**Guanidine 17**		**Antibiotics**		**FICI**
	MIC alone	**MIC in combo.**	**MIC alone**	**MIC in combo.**	
S. aureus MRSA 43300	4 μg/mL	2 μg/mL	OXA 10 μg/mL	0.5 μg/mL	0.550
K. pneumoniae BAA1705	32 μg/mL	16 μg/mL	IMP 20 μg/mL	2 μg/mL	0.600
C. albicans 10231	16 μg/mL	2 μg/mL	VRC 30 μg/mL	0.125 μg/mL	0.129

The data on the antimicrobial activity of all investigated guanidines demonstrate an unusual dependence on the concentration, reflected in lower activities at higher concentrations. These results can be accounted for the known effect of aggregation, demonstrated previously in other studies on guanidines reported in the literature [35]. In particular, a recent report [36] demonstrates reverse micellar formation in dodecylguanidine solutions at concentrations above 5 mM in an unpolar solvent. This phenomenon can be valid in aqueous solutions on incubating tested guanidines with the microbial culture, resulting in micellar formation and lower effective concentration of the active compound on the surface of the bacterial cell and weaker cell wall penetration abilities. This hypothesis has been supported by IR spectroscopy data of compound **16** at different concentrations. The spectra taken in the concentration range matching the antimicrobial evaluations showed an abnormal increase of absorption bands at lower concentrations at wavelengths around 3000 cm^{-1} where –NH and –CH vibrations are usually reflected (Fig. 2). This effect can be definitely connected to an association process due to an aggregation phenomenon at higher concentrations of the tested guanidines.

2.2.3. *In vivo toxicity evaluation*

To investigate the *in vivo* toxicity of guanidine derivatives **16** and **17**, zebrafish embryos were exposed to the chemicals at different concentrations in the range of the active antimicrobial doses. The mortality rate was analyzed at four different developmental stages (24, 48, 72, and 96 hpf) and reported in Fig. 3.

The median lethal concentration values recorded for both **16** and **17** indicate toxicity levels comparable to those of other drugs on the market [37,38]. However, both compounds did not induce embryo mortality at the concentrations used in the checkerboard assay (≤4 μg/mL) that were effective in reducing the MICs of oxacillin and voriconazole against *S. aureus* ATCC 43300 and *C. albicans* ATCC 10231, respectively. In parallel, no mortalities were observed neither in the vehicle group (0.1 % DMSO) nor in the control group (data not shown).

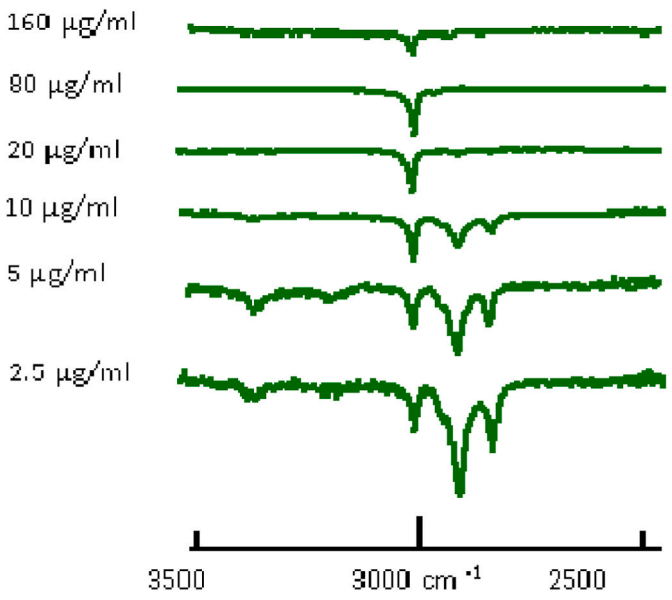

Fig. 2. Sections of the IR spectra of guanidine **16** at different concentrations in $CHCl_3$.

3. Conclusions

In the hope to select novel candidates to treat poly-microbial diseases, in this report, a synthetic route to obtain acylated guanidine derivatives starting from nature-inspired diterpenic carboxylic acids has been developed. This led to obtaining six different guanidines prenylated with labdanic fragments (compounds **13**–**18**) that have been then evaluated for their antimicrobial properties against bacteria strains. Compounds **13**, **14**, **16**–**18** turned out to be strongly active on Gram-positive bacterial strains, including *S. aureus* (two strains) and *S. epidermidis* (two strains) while only compounds **16** and **17** were also active against different strains of the Gram-negative bacteria *K. pneumoniae* and *P. aeruginosa*. Compounds **13**, **14**, **16**–**18** also exhibited antifungal properties against the yeast *C. albicans*.

Overall, guanidines **16** and **17** showed a broader spectrum of antimicrobial properties and were also tested in combination with oxacillin to assess relevant synergistic effects against *S. aureus*. In addition, **16** and **17** also reduced the concentration of the antifungal voriconazole required to inhibit the growth of an azole-resistant strain of *C. albicans*. The results suggest that guanidine **16** and **17** may serve as new lead compounds to face poly-microbial diseases, but also to reduce antibiotic selection pressure in combinations therapy. From this perspective is worth underlining that, when analyzed in combination with oxacillin or voriconazole, both compounds exhibited effective antimicrobial action at concentrations $\leq$ 4 µg/mL, which did not induce mortality *in vivo* in the zebrafish embryonic model. The present study thus encourages to

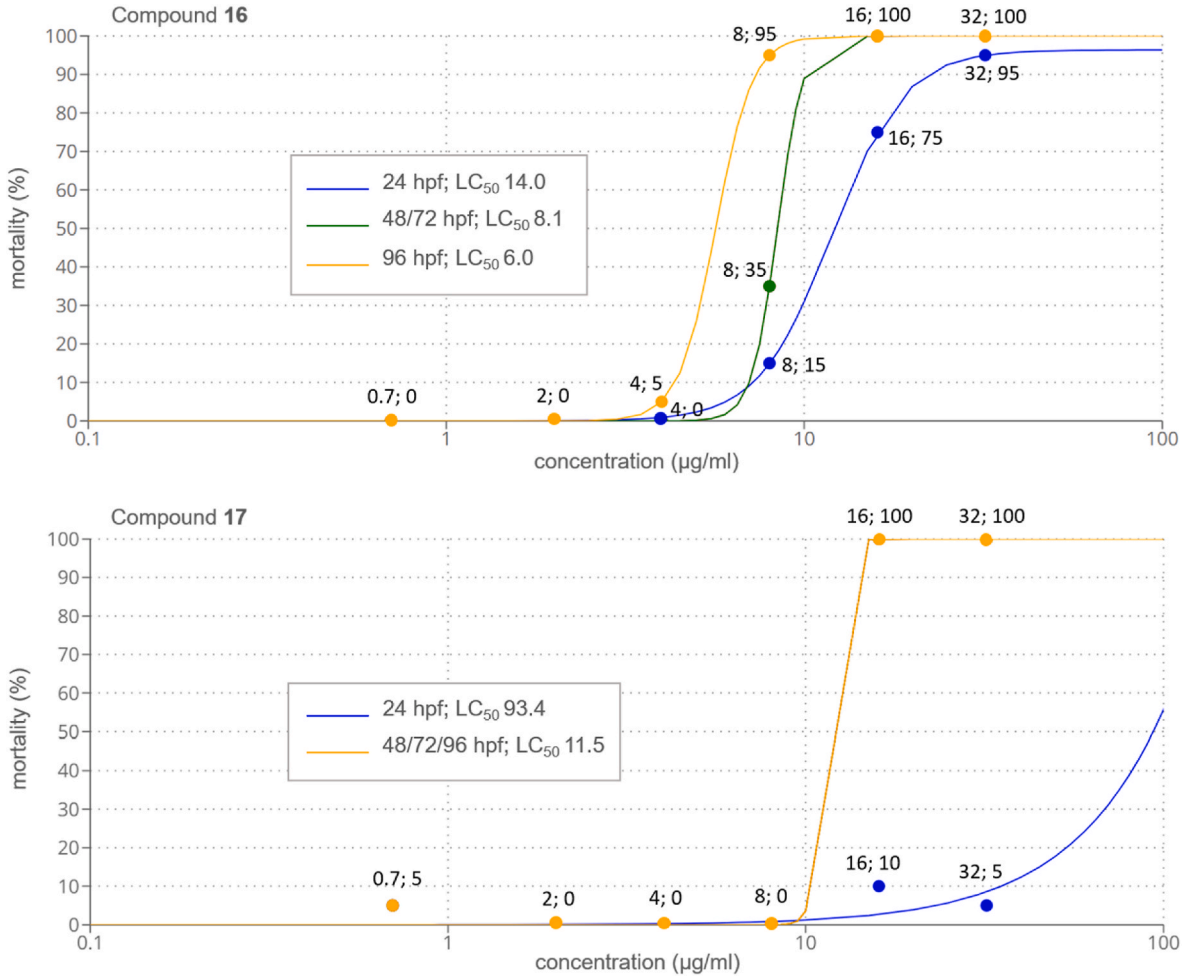

Fig. 3. Acute toxicity on zebrafish embryos after being exposed to increasing doses of compounds **16** and **17** at the developmental stages of 24, 48, 72, and 96 h post fertilization (hpf). LC50 is shown for each stage. Curves/stages completely overlapping are shown in the same color. Close to each point of the curves, x-y pair values are indicated (N = 20 embryos per dose).

examine more thoroughly the pharmacokinetic and pharmacodynamic of guanidines **16** and **17**, as well as to assess their dose-limiting toxicity levels in higher vertebrates.

4. Experimental

4.1. General experimental procedures and reagents

Melting points were measured with a Boethius heating stage. Optical rotations: Jasco-DIP-370 polarimeter; 5-cm cell; in $CHCl_3$. IR spectra: Spectrum-100 F T-IR spectrophotometer (PerkinElmer), with the universal ATR sampling accessory; ν in cm^{-1}.^{1}H and ^{13}C NMR Spectra: Bruker Avance-III spectrometer (400.13 and 100.61 MHz); in $CDCl_3$; δ in ppm rel. to $CHCl_3$ as internal standard (δ (H) 7.26 and δ (C) 77.0), J in Hz. GC/MS: Agilent-7890 A chromatograph; quadrupole MS detector MSD 5975C; HP-5ms capillary column (30 m/0.25 μm). The elemental analysis was performed on a Vario-EL–III–CHNOS Elemental Analyzer.

All reagents were purchased from Merck or Across. Commercial Merck silica gel 60 (70–230 mesh ASTM) was used for column chromatography and Merck pre-coated silica gel plates were used for TLC. The chromatograms were sprayed with 0.1 % solution of cerium (IV) sulfate in 2 N sulfuric acid and heated at 80 °C for 5 min to detect the spots. The work up of the reaction mixtures in organic solvents included the extraction by diethyl ether, washing successively the extract with 20 % H_2SO_4, sat. $NaHCO_3$ and brine to neutral reaction, drying over anhydrous Na_2SO_4, filtration, and solvent removal in vacuum. All moisture sensitive procedures were carried out in dry glassware under N_2 atmosphere.

4.2. Synthetic procedures

*4.2.1. (+)-8α-hydroxe-14,15-bisnorlabdan-13-one (**2**) was obtazned from (−)-sclareol (**1**) following the literature procedure [22]*

*4.2.2. Labda-8(9),13E-dien-15-oic acid (**8**) and labda-8(9),13Z-dien-15-oic acid (**4**) were synthesized according to the literature procedure [23].* *Labda-8(9),13E-dien-15-oic acid (**8**) and labda-8(9),13Z-dien-15-oic acid* (**4**) were synthesized according to the literature procedure [23].

*4.2.3. 15-Norlabdan-8R,13R-diacetoxy-14-oic acid (**5**) was synthesized according to the literature procedure [24]. 15-Norlabdan-8R,13R-diacetoxy-14-oic acid* (**5**) was synthesized according to the literature procedure [24].

*4.2.4. HWE olefination-oxa-Michael reaction of ketone **2***

Trimethylphosphonoacetate (295 mg, 1.62 mmol) was added to a solution of ketone **2** (150 mg, 0.54 mmol) in anhydrous toluene (12 mL) under N_2 atmosphere. The mixture was gradually heated at reflux for 30 min. Sodium metal (44 mg, 1.89 mmol) was dissolved in MeOH (1.2 mL) and the resultant sodium methoxide solution was added slowly *via* syringe to the refluxing reaction mixture. After 2 h the mixture was cooled to r. t. And stirred for 70 h. The resulting mixture was worked up as usual. The crude product (180 mg) was purified by column chromatography (ethyl acetate/petroleum ether mixture, gradient elution) to afford a nonpolar mixture of heterocyclic compounds **11** and **12** (124 mg, ~69 %), followed by polar hydroxy esters **9** and **10** (19 mg, total yield ~11 %). An aliquot of the crude reaction product was analyzed by GC (see entry 10 of Table S1 in Supplementary Material).

4.2.5. Methyl 8α-hydroxylabd-13E-en-15-oate (9)

Colorless crystals, mp: 91–92 °C (Lit [39].: m. p. 88–89 °C); $[\alpha]_D^{27}$ 21.2 (*c* 0.47, CHCl3). Lit [39].: $[\alpha]_D^{20}$ 13.7 (*c* 0.71, $CHCl_3$). IR (ν, cm^{-1}): 1147, 1223, 1364, 1387, 1435, 1645, 1720, 2924, 3534.^{1}H NMR (400.13 MHz, $CDCl_3$) δ: 0.78 (s, 3H, H-19), 0.79 (s, 3H, H-20), 0.87 (s, 3H, H-18), 0.92 (dd, J = 12.0, 2.2 Hz, 1H, H-5), 0.94 (m, 1H, H-1ax), 1.05 (t, J = 3.9 Hz, 1H, H-9), 1.14 (m, 1H, H-3ax), 1.15 (d, J = 0.3 Hz, 3H, H-17), 1.26 (m, 1H, H-6ax), 1.37 (m, 1H, H-3eq), 1.40 (m, 2H, H-7ax and H-11ax), 1.43 (m, 1H, H-2eq), 1.57 (m, 1H, H-2ax), 1.59 (m, 1H, H-11eq), 1.63 (m, 1H, H-1eq), 1.65 (m, 1H, H-6eq), 1.86 (dt, J = 12.2, 3.2 Hz, 1H, H-7eq), 2.17 (d, J = 1.2 Hz, 3H, H-16), 2.18 (m, 1H, H-12ax), 2.28 (m, 1H, H-12eq), 3.68 (s, 3H, OMe), 5.68 (m, 1H, H-14). ^{13}C NMR (100.61 MHz, $CDCl_3$) δ: 15.4 (q, C-20), 18.4 (t, C-2), 19.1 (q, C-16), 20.5 (t, C-6), 21.5 (q, C-19), 23.6 (t, C-11), 24.0 (q, C-17), 33.2 (s, C-4), 33.4 (q, C-18), 39.2 (s, C-10), 39.8 (t, C-1), 41.9 (t, C-3), 44.3 (t, C-12), 44.7 (t, C-7), 50.8 (q, OMe), 56.1 (d, C-5), 61.4 (d, C-9), 74.2 (s, C-8), 114.7 (d, C-14), 161.3 (s, C-13), 167.4 (s, C-15). Anal. Calc. For $C_{21}H_{36}O_3$: C, 74.95; H, 10.78. Found: C, 74.97; H, 10.75.

4.2.6. Methyl 8α-hydroxylabd-13Z-en-15-oate (10)

Colorless crystals, mp: 135–136 °C (Lit [39].: m. p. 132–134 °C); $[\alpha]_D^{25}$ 24.8 (*c* 0.43, CHCl3). Lit [39].: $[\alpha]_D^{20}$ 34.6 (*c* 0.68, $CHCl_3$). IR (ν, cm^{-1}): 1145, 1174, 1237, 1376, 1388, 1439, 1641, 1702, 2919, 3530.^{1}H NMR (400.13 MHz, $CDCl_3$) δ: 0.76 (s, 3H, H-20), 0.78 (s, 3H, H-19), 0.87 (s, 3H, H-18), 0.92 (dd, J = 12.2, 2.2 Hz, 1H, H-5), 0.94 (m, 1H, H-1ax), 1.14 (m, 1H, H-3ax), 1.16 (m, 1H, H-9), 1.18 (br. s, 3H, H-17), 1.24 (m, 1H, H-6ax), 1.37 (dm, J = 13.1 Hz, 1H, H-3eq), 1.44 (m, 2H, H-2eq and H-7ax), 1.46 (m, 2H, H-11), 1.58 (m, 1H, H-2ax), 1.64 (m, 1H, H-6eq), 1.68 (m, 1H, H-1eq), 1.86 (dt, J = 12.4, 3.2 Hz, 1H, H-7eq), 1.91 (d, J = 1.3 Hz, 3H, H-16), 2.21 (m, 1H, H-12ax), 2.93 (m, 1H, H-12eq), 3.66 (s, 3H, OMe), 5.66 (m, 1H, H-14). ^{13}C NMR (100.61 MHz, CDCl3) δ: 15.5 (q, C-20), 18.5 (t, C-2), 20.3 (t, C-6), 21.5 (q, C-19), 24.2 (q, C-17), 24.3 (t, C-11), 25.6 (q, C-16), 33.3 (s, C-4), 33.4 (q, C-18), 37.5 (t, C-12), 39.9 (s, C-10), 39.4 (t, C-1), 42.0 (t, C-3), 43.3 (t, C-7), 51.1 (q, OMe), 56.1 (d, C-5), 61.7 (d, C-9), 73.9 (s, C-8), 115.2 (d, C-14), 161.9 (s, C-13), 167.0 (s, C-15). Anal. Calc. For $C_{21}H_{36}O_3$: C, 74.95; H, 10.78. Found: C, 74.86; H, 10.85.

*4.2.7. Synthesis of entgomeric acids (**6**) and (**7**)*

The mixture of the esters **11** and **12** (124 mg, 0.37 mmol) was dissolved in MeOH (2 mL) and 10 % KOH/MeOH solution (3 mL) was added. The reaction was heated at reflux for 3 h and worked up as usual. The crude product (121 mg) was purified on a SiO_2 chromatography column (ethyl acetate/petroleum ether as eluent) to yield in order of increasing polarity pure labd-8,13(*R*)-epoxy-15-oic acid (**6**) (53 mg, ~43 %) and labd-8,13(*S*)-epoxy-15-oic acid (**7**) (34 mg, ~28 %).

4.2.8. Labdan-8,13(R)-epoxy-15-oic acid (6)

Colorless crystals, mp: 113–114 °C (Lit [25]. for enantiomer: m. p. 113–115 °C); $[\alpha]_D^{20}$ 26.6 (*c* 2.1, $CHCl_3$), Lit [25]. for enantiomer: $[\alpha]_D^{20}$ -34.0 (*c* 0.13 $CHCl_3$). IR (ν, cm^{-1}): 1078, 1097, 1115, 1254, 1377, 1444, 1708, 2924.^{1}H NMR (400.13 MHz, $CDCl_3$) δ: 0.77 (s, 3H, H-20), 0.78 (s 3H, H-19), 0.85 (s, 3H, H-18), 0.86 (m, 1H, H-1ax), 0.95 (dd, J = 12.2, 2.5 Hz, 1H, H-5), 1.13 (td, J = 13.4, 4.2 Hz, 1H, H-3ax), 1.22 (m, 1H, H-9), 1.29 (m, 1H, H-6ax), 1.36 (br. s, 6H, H-17 and H-16), 1.37 (m, 1H, H-3eq), 1.40 (m, 1H, H-7ax), 1.46 (m, 1H, H-2eq), 1.52 (m, 1H, H-11ax), 1.60 (m, 2H, H-2ax and H-12ax), 1.61 (m, 1H, H-1eq), 1.62 (m, 1H, H-11eq), 1.70 (m, 1H, H-6eq), 1.74 (m, 1H, H-12eq), 1.87 (dt, J = 11.7, 3.0 Hz, 1H, H-7eq), 2.39 (d, J = 15.6 Hz, 1H, H-14a), 2.54 (d, J = 15.6 Hz, 1H, H-14 b). ^{13}C NMR (100.61 MHz, $CDCl_3$) δ: 14.9 (t, C-11), 15.7 (q, C-20), 18.4 (t, C-2), 19.7 (t, C-6), 21.2 (q, C-19), 24.4 (q, C-17), 27.3 (q, C-16), 33.18 (q, C-18), 33.23 (s, C-4), 36.5 (t, C-12), 37.0 (s, C-10), 38.9 (t, C-1), 41.9 (t, C-3), 42.6 (t, C-7), 49.6 (t, C-14), 56.2 (d, C-5), 57.7 (d, C-9), 73.5 (s, C-13), 78.6 (s, C-8), 171.4 (s, C-15). GC-MS: 322, 307, 289, 261, 245, 229. Anal. Calc. For $C_{20}H_{34}O_3$: C, 74.49; H, 10.63. Found: C, 74.38; H, 10.69. Methylation of pure acid **6** with an ethereal solution of diazomethane provided crude methyl *ent*-gomeroate (**11**) which was purified by column chromatography (0.5 g SiO_2; ethyl acetate/petroleum ether mixture, gradient elution) to afford pure ester **11**.

4.2.9. Methyl labdan-8,13(R)-epoxy-15-oate (11)

Colourless crystals, mp: 112–113 °C (Lit [25]. for enantiomer: m. p.

106–107 °C); $[\alpha]_D^{28}$ 16.5 (*c* 1.2, $CHCl_3$). Lit [25]. for enantiomer: $[\alpha]_D^{20}$ − 22.0 (*c* 1.46, $CHCl_3$). IR (ν, cm^{-1}): 1077, 1097, 1117, 1207, 1378, 1441, 1729, 2926.^{1}H NMR (400.13 MHz, $CDCl_3$) δ: 0.75 (s, 3H, H-20), 0.78 (s 3H, H-19), 0.84 (s, 3H, H-18), 0.86 (m, 1H, H-1ax), 0.92 (dd, J = 12.0, 2.3 Hz, 1H, H-5), 1.13 (m, 1H, H-3ax), 1.15 (dd, J = 12.1, 3.0 Hz, 1H, H-9), 1.23 (m, 1H, H-6ax), 1.26 (m, 1H, H-7ax), 1.27 (s, 3H, H-17), 1.33 (s, 3H, H-16), 1.36 (m, 1H, H-3eq), 1.43 (m, 1H, H-2eq), 1.44 (m, 1H, H-11ax), 1.56 (m, 1H, H-11eq), 1.58 (m, 1H, H-2ax), 1.60 (m, 2H, H-1eq and H-6eq), 1.69 (m, 1H, H-12ax), 1.73 (m, 1H, H-7eq), 1.94 (td, J = 12.4, 5.2 Hz, 1H, H-12ax), 2.37 (d, J = 13.2 Hz, 1H, H-14a) 2.48 (d, J = 13.2 Hz, 1H, H-14 b), 3.66 (s, 3H, OMe). ^{13}C NMR (100.61 MHz, $CDCl_3$) δ: 15.3 (t, C-11), 15.7 (q, C-20), 18.6 (t, C-2), 19.9 (t, C-6), 21.3 (q, C-19), 24.7 (q, C-17), 28.2 (q, C-16), 33.3 (s, C-4), 33.3 (q, C-18), 35.8 (t, C-12), 36.9 (s, C-10), 39.1 (t, C-1), 42.2 (t, C-3), 43.0 (t, C-7), 49.5 (t, C-14), 51.2 (q, OMe), 56.4 (d, C-5), 57.4 (d, C-9), 72.3 (s, C-13), 75.4 (s, C-8), 171.6 (s, C-15). GC-MS: 336, 321, 303, 289, 263, 245, 229. Anal. Calc. For $C_{21}H_{36}O_3$: C, 74.95; H, 10.78. Found: C, 74.99; H, 10.72.

4.2.10. Labdan-8,13(S)-epoxy-15-oic acid (7)

Colorless crystals, mp: 130–131 °C (Lit [25]. for enantiomer: m. p. 127–129 °C); $[\alpha]_D^{20}$ 36.9 (*c* 1.07, $CHCl_3$). Lit [25]. for enantiomer: $[\alpha]_D^{20}$ − 20.0 (*c* 0.60, $CHCl_3$). IR (ν, cm-1): 1078, 1097, 1224, 1377, 1458, 1706, 2938.^{1}H NMR (400.13 MHz, CDCl3) δ: 0.78 (s, 3H, H-20), 0.79 (s, 3H, H-19), 0.86 (s, 3H, H-18), 0.87 (m, 1H, H-1ax), 0.96 (dd, J = 12.4, 2.4 Hz, 1H, H-5), 1.14 (td, J = 13.4, 4.1 Hz, 1H, H-3ax), 1.26 (m, 1H, H-6ax), 1.30 (s, 3H, H-16), 1.33 (m, 1H, H-9), 1.35 (s, 3H, H-17), 1.37 (m, 1H, H-3eq), 1.45 (m, 3H, H-2eq, H-11ax and H-7ax), 1.60 (m, 2H, H-1eq and H-2ax), 1.63 (m, 2H, H-11eq and H-12ax), 1.68 (m, 1H, H-6eq), 1.82 (m, 1H, H-7eq), 1.85 (m, 1H, H-12eq), 2.32 (d, J = 16.5 Hz, 1H, H-14a) 2.87 (d, J = 16.5 Hz, 1H, H-14 b). ^{13}C NMR (100.61 MHz, $CDCl_3$) δ: 14.9 (t, C-11), 15.6 (q, C-20), 18.4 (t, C-2), 19.8 (t, C-6), 21.2 (q, C-19), 23.6 (q, C-17), 30.4 (q, C-16), 33.2 (s, C-4), 33.3 (q, C-18), 36.6 (t, C-12), 37.1 (s, C-10), 39.0 (t, C-1), 42.0 (t, C-3), 43.0 (t, C-7), 45.8 (t, C-14), 55.9 (d, C-9), 56.3 (d, C-5), 72.3 (s, C-13), 78.2 (s, C-8), 172.6 (s, C-15). GC-MS: 322, 307, 289, 261, 245, 229. Anal. Calc. For $C_{20}H_{34}O_3$: C, 74.49; H, 10.63. Found: C, 74.40; H, 10.68. Methylation of pure acid (**7**) with an ethereal solution of diazomethane provided crude methyl *ent*-gomeroate (**12**) which was purified by column chromatography (0.5 g SiO_2; ethyl acetate/petroleum ether mixture, gradient elution) to afford pure ester **12**.

4.2.11. Methyl labdan-8,13(S)-epoxy-15-oate (12)

Colorless amorphous gum; $[\alpha]_D^{28}$ 24.3 (*c* 0.6, $CHCl_3$). IR (ν, cm-1): 1078, 1098, 1216, 1376, 1458, 1737, 2926.^{1}H NMR (400.13 MHz, $CDCl_3$) δ: 0.76 (s, 3H, H-20), 0.79 (s, 3H, H-19), 0.85 (s, 3H, H-18), 0.86 (m, 1H, H-1ax), 0.94 (dd, J = 12.1, 2.3 Hz, 1H, H-5), 1.13 (td, J = 13.6, 4.2 Hz, 1H, H-3ax), 1.23 (m, 1H, H-9), 1.25 (br. s, 6H, H-16 and H-17), 1.27 (m, 1H, H-6ax), 1.36 (m, 2H, H-3eq and H-7ax), 1.42 (m, 1H, H-2eq), 1.45 (m, 2H, H-11ax and H-12ax), 1.56 (m, 1H, H-11eq), 1.58 (m, 1H, H-2ax), 1.61 (m, 1H, H-1eq), 1.64 (m, 1H, H-6eq), 1.76 (dt, J = 11.8, 3.1 Hz, 1H, H-7eq), 2.11 (m, 1H, H-12eq), 2.56 (d, J = 13.3 Hz, 1H, H-14a) 2.72 (d, J = 13.3 Hz, 1H, H-14 b), 3.64 (s, 3H, OMe). ^{13}C NMR (100.61 MHz, $CDCl_3$) δ: 15.2 (t, C-11), 15.6 (q, C-20), 18.6 (t, C-2), 19.9 (t, C-6), 21.3 (q, C-19), 24.6 (q, C-17), 30.6 (q, C-16), 33.27 (s, C-4), 33.3 (q, C-18), 36.5 (t, C-12), 37.0 (s, C-10), 39.2 (t, C-1), 42.2 (t, C-3), 43.3 (t, C-7), 45.9 (t, C-14), 51.3 (q, OMe), 56.5 (d, C-5), 57.4 (d, C-9), 72.1 (s, C-13), 75.5 (s, C-8), 171.9 (s, C-15). GC-MS: 336, 321, 303, 289, 263, 245, 229. Anal. Calc. For $C_{21}H_{36}O_3$: C, 74.95; H, 10.78. Found: C, 74.89; H, 10.82.

4.2.12. Synthesis of prenylated guanidines

The general procedure involves carboxyl group activation and interaction with guanidine-base. Synthesis of compound **17** is given as an example.

To a solution of the substrate **7** (100 mg, 0.301 mmol, 1 equiv) in dry DMF (0.94 mL) under nitrogen was added CDI (73 mg, 0.452 mmol, 1.5 equiv) and the resulting mixture was stirred at room temperature until the initial substrate was completely consumed (monitored by TLC, approx. 48 h). Sodium metal (10 mg, 0.452 mmol, 1.5 equiv) was dissolved in dry methanol (0.3 mL) and treated with a guanidine hydrochloride (43 mg, 0.452 mmol, 1.5 equiv). The obtained mixture was stirred for 30 min at room temperature. After the solvent evaporation the residue was dried under reduced pressure during 1 h then dissolved in dry DMF (1 mL). Activated acid was added dropwise to the solution of guanidine base in DMF and stirred at room temperature for 3 h (monitored by TLC). On the disappearance of starting material (activated carboxylic acid) the mixture was diluted with 5 mL of water and extracted with ethyl acetate. The combined organic phase was washed successively with brine, sat. Aq. NH_4Cl and brine, dried over sodium sulfate and evaporated in vacuo. The crude product was purified by column chromatography (CC) on silica gel using methanol-dichloromethane mixture as eluent to give the corresponding monoacylguanidine **17** (54 mg, 48 %).

4.2.13. Labdan-8,13(S)-epoxy-15-oyl guanidine (17)

White powder, mp: 214-214 °C; $[\alpha]_D^{28}$ 36.95 (*c* 0.21, $CHCl_3$). IR (ν, cm^{-1}): 735, 1096, 1122, 1215, 1377, 1457, 1575, 1695, 2925, 3348.^{1}H NMR (400.13 MHz, $CDCl_3$) δ: 0.77 (s, 3H, H-20), 0.78 (s, 3H, H-19), 0.85 (s, 3H, H-18), 0.86 (m, 1H, H-1ax), 0.93 (dd, J = 12.1, 2.1 Hz, 1H, H-5), 1.13 (td, J = 13.0, 3.8 Hz, 1H, H-3ax), 1.25 (m, 1H, H-6ax), 1.28 (s, 3H, H-17), 1.29 (m, 1H, H-9), 1.31 (s, 3H, H-16), 1.37 (m, 2H, H-3eq and H-7ax), 1.42 (m, 1H, H-2eq), 1.50 (m, 2H, H-11ax and H-12ax), 1.59 (m, 3H, H-1eq, H-2ax and H-11eq), 1.64 (m, 1H, H-6eq), 1.80 (dt, J = 12.0, 2.8 Hz, 1H, H-7eq), 2.01 (m, 1H, H-12eq), 2.69 (d, J = 13.9 Hz, 1H, H-14a) 2.74 (d, J = 13.9 Hz, 1H, H-14 b), 8.45 (br. s, 3H, –NH and $–NH_2$), 11.39 (br. s, 1H, =NH). ^{13}C NMR (100.61 MHz, $CDCl_3$) δ: 15.1 (t, C-11), 15.5 (q, C-20), 18.5 (t, C-2), 19.9 (t, C-6), 21.3 (q, C-19), 24.8 (q, C-17), 30.4 (q, C-16), 33.2 (s, C-4), 33.3 (q, C-18), 35.9 (t, C-12), 37.0 (s, C-10), 39.1 (t, C-1), 42.1 (t, C-3), 43.2 (t, C-7), 49.3 (t, C-14), 56.2 (d, C-9), 56.5 (d, C-5), 72.3 (s, C-13), 76.0 (s, C-8), 156.2 (s, C-1′), 173.6 (s, C-15). Anal. Calc. For $C_{21}H_{37}N_3O_2$: C, 69.38; H, 10.26; N, 11.56. Found: C, 69.43; H, 10.32; N, 11.61.

4.2.14. Labda-8(9),13Z-dien-15-oyl guanidine (13)

The acid **3** (188 mg) was converted to guanidine **13** (97 mg, 46 %) according to the general procedure. White powder, mp: 123–124 °C; $[\alpha]_D^{28}$ 40.4 (*c* 0.22, $CHCl_3$). IR (ν, cm^{-1}): 736, 1153, 1222, 1366, 1443, 1578, 1612, 1693, 2925, 3346.^{1}H NMR (400.13 MHz, $CDCl_3$) δ: 0.82 (s, 3H, H-19), 0.88 (s, 3H, H-18), 0.93 (s, 3H, H-20), 1.09 (m, 1H, H-5), 1.14 (m, 2H, H-3ax and H-1ax), 1.40 (m, 2H, H-2eq and H-3eq), 1.49 (m, 1H, H-2ax), 1.56 (s, 3H, H-17), 1.62 (m, 2H, H-6), 1.78 (m, 1H, H-1eq), 1.95 (m, 2H, H-7), 2.04 (m, 1H-11ax), 2.15 (m, 1H, H-11eq), 2.23 (m, 2H, H-12), 2.24 (d, J = 0.7 Hz, 3H, H-16), 5.85 (br. s, 1H, H-14), 8.36 (br. s, 3H, –NH and $–NH_2$), 11.23 (br. s, 1H, =NH). ^{13}C NMR (100.61 MHz, $CDCl_3$) δ: 19.1 (t, C-2 and C-6), 19.6 (q, C-17), 19.8 (q, C-16), 20.2 (q, C-20), 21.7 (q, C-19), 26.2 (t, C-11), 33.3 (s, C-4), 33.33 (q, C-18), 33.8 (t, C-7), 37.2 (t, C-1), 39.1 (s, C-10), 41.8 (t, C-3), 42.3 (t, C-12), 51.9 (d, C-5), 115.3 (d, C-14), 127.1 (s, C-8), 139.2 (s, C-9), 157.1 (s, C-1′) 167.3 (s, C-15), 167.4 (s, C-13). Anal. Calc. For $C_{21}H_{35}N_3O$: C, 73.00; H, 10.21; N, 12.16. Found: C, 72.95; H, 10.30; N, 12.19.

4.2.15. Labda-8(9),13E-dien-15-oyl guanidine (14)

The acid **4** (237 mg) was converted to guanidine **14** (129 mg, 48 %) according to the general procedure. White powder, mp: 126–127 °C; $[\alpha]_D^{28}$ 43.9 (*c* 0.23, $CHCl_3$). IR (ν, cm^{-1}): 738, 1165, 1223, 1387, 1442, 1576, 1613, 1692, 2927, 3344.^{1}H NMR (400.13 MHz, $CDCl_3$) δ: 0.81 (s, 3H, H-19), 0.86 (s, 3H, H-18), 0.92 (s, 3H, H-20), 1.09 (m, 1H, H-5), 1.12 (m, 2H, H-1ax and H-3ax), 1.39 (m, 2H, H-2eq and H-3eq), 1.47 (m, 1H, H-2ax), 1.55 (s, 3H, H-17), 1.61 (m, 2H, H-6), 1.78 (dm, J = 12.3 Hz, 1H, H-1eq), 1.96 (m, 2H, H-7), 2.02 (m, 1H, H-11ax), 2.14 (m, 1H, H-11eq), 2.20 (m, 2H, H-12), 2.23 (s, 3H, H-16), 5.84 (br. s, 1H, H-14), 8.36 (br. s, 4H, $–NH_2$). ^{13}C NMR (100.61 MHz, $CDCl_3$) δ: 19.0 (t, C-2 and C-6), 19.5

(q, C-17), 19.7 (q, C-16), 20.2 (q, C-20), 21.7 (q, C-19), 26.1 (t, C-11), 33.27 (s, C-4), 33.3 (q, C-18), 33.7 (t, C-7), 37.1 (t, C-1), 39.1 (s, C-10), 41.7 (t, C-3), 42.3 (t, C-12), 51.9 (d, C-5), 115.3 (d, C-14), 127.1 (s, C-8), 139.1 (s, C-9), 156.9 (s, C-1′), 167.3 (s, C-13 and C-15). Anal. Calc. For $C_{21}H_{35}N_3O$: C, 73.00; H, 10.21; N, 12.16. Found: C, 72.98; H, 10.32; N, 12.21.

4.2.16. Synthesis of N-[Labda-8 (9),13E-dien-15-oyl]-N′-senecioyl guanidine (15)

To a solution of 3,3-dimethylacrylic acid (29 mg, 289 mmol) in *N*-methylpyrrolidone (NMP) (1.5 mL) 2-chloro-1-methylpyridinium iodide (CMPI) (84 mg, 0.330 mmol) was added and the resulting mixture was stirred for 1 h at 50 °C. The reaction was cooled to r. t. And a solution of monoacylguanidine **14** (95 mg, 0.275 mmol) in NMP (0.9 mL) and DIPEA (0.24 mL, 1.375 mmol) were added. The mixture was stirred for 48 h, which than was quenched by addition of water (6 mL) and extracted with EtOAc. The combined org. Phase was washed with brine, dried over sodium sulfate and evaporated in vacuo. The crude product was submitted to CC (silica gel 6.0 g), increasing gradient of MeOH in dichloromethane) giving **15** (61 mg, 52 %). White powder, mp: 74–75 °C; $[\alpha]_D^{28}$ 24.33 (*c* 2.14, $CHCl_3$). IR (δ, cm^{-1}): 733, 1140, 1222, 1358, 1442, 1525, 1622, 2927, 3339.1H NMR (400.13 MHz, $CDCl_3$) δ: 0.82 (s, 3H, H-19), 0.88 (s, 3H, H-18), 0.93 (s, 3H, H-20), 1.09 (m, 1H, H-5), 1.14 (m, 2H, H-1ax and H-3ax), 1.39 (m, 2H, H-2eq and H-3eq), 1.46 (m, 1H, H-2ax), 1.56 (s, 3H, H-17), 1.62 (m, 2H, H-6), 1.78 (m, 1H, H-1eq), 1.89 (s, 3H, H-4″), 1.95 (m, 2H, H-7), 2.01 (m, 1H, H-11ax), 2.14 (m, 1H, H-11eq), 2.16 (m, 2H, H-12), 2.19 (d, $J = 0.6$ Hz, 3H, H-5″), 2.21 (d, $J = 0.7$ Hz, 3H, H-16), 5.74 (m, 1H, H-2″), 5.76 (br. s, 1H, H-14), 8.77 (br. s, 2H, NH). ^{13}C NMR (100.61 MHz, $CDCl_3$) δ: 19.1 (t, C-2 and C-6), 19.2 (q, C-16), 19.5 (q, C-17), 20.2 (q, C-20), 20.4 (q, C-5″), 21.7 (q, C-19), 26.4 (t, C-11), 27.8 (q, C-4″), 33.3 (s, C-4 and C-18), 33.7 (t, C-7), 37.1 (t, C-1), 39.1 (s, C-10), 41.8 (t, C-3), 41.9 (t, C-12), 51.9 (d, C-5), 119.8 (d, C-14), 120.6 (d, C-2″), 126.7 (s, C-8), 139.5 (s, C-9), 157.2 (s, C-3″), 159.1 (s, C-1′), 161.2 (s, C-13), 173.2 (s, C-1″), 174.4 (s, C-15). Anal. Calc. For $C_{26}H_{41}N_3O_2$: C, 73.03; H, 9.66; N, 9.83. Found: C, 72.97; H, 9.73; N, 9.91.

4.2.17. Labdan-8,13(R)-epoxy-15-oyl guanidine (16)

The acid **6** (213 mg) was converted to guanidine **16** (107 mg, 45 %) according to the general procedure. White powder, mp: 128–130 °C; $[\alpha]_D^{28}$ − 13.35 (*c* 0.24, $CHCl_3$). IR (ν, cm^{-1}): 735, 1097, 1114, 1245, 1377, 1444, 1584, 1696, 2924, 3347.^{1}H NMR (400.13 MHz, $CDCl_3$) δ: 0.74 (s, 3H, H-20), 0.77 (s 3H, H-19), 0.84 (s, 3H, H-18), 0.86 (m, 1H, H-1ax), 0.92 (dd, $J = 12.2$, 2.1 Hz, 1H, H-5), 1.11 (m, 1H, H-9), 1.14 (m, 1H, H-3ax), 1.24 (m, 1H, H-6ax), 1.26 (s, 3H, H-17), 1.30 (m, 1H, H-7ax), 1.34 (s, 3H, H-16), 1.36 (m, 1H, H-3eq), 1.42 (m, 1H, H-2eq), 1.49 (m, 1H, H-11ax), 1.56 (m, 1H, H-11eq), 1.57 (m, 1H, H-2ax), 1.58 (m, 1H, H-1eq), 1.61 (m, 1H, H-6eq), 1.71 (m, 2H, H-12), 1.75 (m, 1H, H-7eq), 2.46 (d, $J = 13.3$ Hz, 1H, H-14a) 2.51 (d, $J = 13.3$ Hz, 1H, H-14 b), 7.16 (s, 1H, –NH), 8.05 (br. s, 3H, =NH and $-NH_2$). ^{13}C NMR (100.61 MHz, $CDCl_3$) δ: 15.1 (t, C-11), 15.7 (q, C-20), 18.5 (t, C-2), 19.7 (t, C-6), 21.3 (q, C-19), 24.6 (q, C-17), 27.8 (q, C-16), 33.30 (q, C-4 and C-18), 36.6 (t, C-12), 36.7 (s, C-10), 38.9 (t, C-1), 42.0 (t, C-3), 42.8 (t, C-7), 52.8 (t, C-14), 56.2 (d, C-5), 57.6 (d, C-9), 72.8 (s, C-13), 76.1 (s, C-8), 156.0 (s, C-1′), 173.6 (s, C-15). Anal. Calc. For $C_{21}H_{37}N_3O_2$: C, 69.38; H, 10.26; N, 11.56. Found: C, 69.41; H, 10.31; N, 11.59.

4.2.18. 15-Norlabdan-8R,13R-diacetoxy-14-oyl guanidine (18)

The acid **5** (190 mg) was converted to guanidine **18** (99 mg, 47 %) according to the general procedure. White powder, mp: 128–129 °C; $[\alpha]_D^{28}$ − 12.6 (*c* 0.18, $CHCl_3$). IR (ν, cm^{-1}): 735, 1019, 1131, 1187, 1249, 1368, 1444, 1525, 1597, 1723, 2927, 3370.^{1}H NMR (400.13 MHz, $CDCl_3$) δ: 0.76 (s, 3H, H-19), 0.81 (s, 3H, H-20), 0.85 (s, 3H, H-18), 0.95 (m, 2H, H-1ax and H-5), 1.13 (dt, $J = 13.2$, 3.8 Hz, 1H, H-3ax), 1.24 (m, 1H, H-11ax), 1.29 (m, 2H, H-6), 1.36 (m, 1H, H-3eq), 1.42 (m, 1H, H-2eq), 1.43 (s, 3H, H-17), 1.47 (m, 1H, H-9), 1.54 (m, 2H, H-1eq and H-2ax), 1.58 (s, 3H, H-16), 1.64 (m, 1H, H-11eq), 1.67 (m, 1H, H-7ax), 1.91 (m, 1H, H-12ax), 1.97 (s, 3H, Me-OAc), 2.10 (s, 3H, Me-OAc), 2.14 (m, 1H, H-12ax), 2.62 (m, 1H, H-7eq), 8.29 (br. s, 4H, $-NH_2$). ^{13}C NMR (100.61 MHz, $CDCl_3$) δ: 15.7 (q, C-20), 18.3 (t, C-2), 19.1 (t, C-6), 19.9 (t, C-11), 20.5 (q, C-17), 21.4 (q, C-16 or C-19), 21.44 (q, C–OAc), 22.8 (q, C–OAc), 33.1 (s, C-4), 33.3 (q, C-18), 38.8 (t, C-7), 39.4 (s, C-10), 39.5 (t, C-1), 39.6 (t, C-12), 41.8 (t, C-3), 55.9 (d, C-5), 58.6 (d, C-9), 83.1 (s, C-13), 87.8 (s, C-8), 158.8 (s, C-1′), 170.3 (s, *C*-OAc), 170.4 (s, *C*-OAc), 178.4 (s, C-14). Anal. Calc. For $C_{24}H_{41}N_3O_5$: C, 63.83; H, 9.15; N, 9.30. Found: C, 63.78; H, 9.21; N, 9.34.

4.3. Microbial strains and reagents

S. aureus ATCC 29213, *S. aureus* ATCC 43300 (methicillin resistant strain, MRSA), *S. epidermidis* ATCC 12228, *S. epidermidis* ATCC 35984 (biofilm producer), *Klebsiella pneumoniae* ATCC 13883, *K. pneumoniae* BAA1705 (carbapenem resistant strain), *Pseudomonas aeruginosa* ATCC 27853, *P. aeruginosa* PAO1 (ATCC BAA-47-B1), *Candida albicans* ATCC 90028, *C. albicans* ATCC 10231 (azole resistant strain) were obtained from the American Type Culture Collection (Rockville, MD). Antibiotics were purchased from Sigma-Aldrich (Milan, Italy).

4.4. Antibacterial susceptibility testing

The compounds were added to bacterial suspension in each well yielding a final cell concentration of 1×10^6 CFU/mL and a final compound concentration ranging from 0.5 to 128 μg/mL. DMSO control wells were set to contain bacteria in Mueller–Hinton broth plus the amount of vehicle (DMSO) used to dilute each compound. Positive controls included vancomycin (VAN, 2 μg/mL; 4 μg/mL for coagulase-negative *S. epidermidis*), oxacillin (OXA, 2 μg/mL), tobramycin (TOB, 2 μg/mL), gentamycin (GEN, 4 μg/mL), and imipenem (IPM, 4 μg/mL). In each test, negative control wells (sterility control) containing Mueller–Hinton medium (MH) only, was added. All antibiotic concentrations reported are according to breakpoint values reported in the EUCAST v.12.0 (The European Committee on Antimicrobial Susceptibility Testing. Breakpoint tables for interpretation of MICs and zone diameters. Version 12.0, 2022. http://www.eucast.org") [32]. The minimal inhibitory concentration (MIC) of all the compounds were determined in MH by the broth microdilution assay, following the procedure already described [40]. The MIC was defined as the lowest concentration of drug that caused a total inhibition of microbial growth (absence of turbidity) after 24 h incubation time at 37 °C. Medium turbidity was measured by a microtiter plate reader (Thermo Scientific Multiskan GO, Waltham, MA USA) at 595 nm. Minimum bactericidal concentration (MBC) was defined as the concentration that caused ≥ 3log10 reduction in colony count from the starting inoculum plated on TSA, incubated for 24 h at 37 °C. All the tests were conducted at least three times using independent cell suspensions.

4.5. Antifungal susceptibility testing

The antifungal activity of compounds was determined on *Candida albicans* by using a standardized broth microdilution method (Clinical and Laboratory Standards Institute (CLSI). Performance Standards for Antifungal Susceptibility Testing of Yeasts. 3rd ed. CLSI supplement M27M44 S, 2022) [33]. Briefly, cell suspension was adjusted to 3×10^3 CFU/mL in RPMI 1640 medium (Sigma) supplemented with 0.2 % (w/v) glucose. One hundred microliter aliquots of these cell suspensions were dispensed into 96-well microtiter plates. Compounds were serially diluted using RPMI 1640 medium and added to the wells at a final concentration ranging from 0.12 to 128 μg/mL, and the plate was incubated for 48 h at 37 °C. Amphotericin B (AMB, 2 μg/mL) and voriconazole (VRC, 0.12 μg/mL) were chosen as the positive controls. Minimum fungicidal concentration (MFC) was defined as the concentration that caused ≥ 3log10 reduction in colony count from the starting

inoculum plated on SDA, incubated for 48 h at 37 °C. All the tests were conducted at least three times using independent cell suspensions.

4.6. Checkerboard testing method

The interaction between compounds **16** or **17** and oxacillin, imipenem, and voriconazole against MRSA, *K. pneumoniae* BAA1705, and *C. albicans* 10231, respectively, was evaluated by the checkerboard method in 96-well microtiter plates containing Mueller–Hinton broth. Briefly, compounds **16** or **17** and antibiotics were serially diluted along the y and x axes, respectively. The final concentration ranged from 0.03 to 32 μg/mL (0.03, 0.06, 0.12, 0.25, 0.5, 1, 2, 4, 8, 16, 32) for antibiotics and from 0.5 to 8 μg/mL (0.5, 1, 2, 4, 8) for **16** and **17**. The checkerboard plates were inoculated with bacteria at an approximate concentration of 10^5 × CFU/mL and incubated at 37 °C for 24 h, following which bacterial growth was assessed visually and the turbidity measured by microplate reader at 595 nm. The synergistic effects of the compounds **16** or **17** combination with the antibiotics were based on a calculation of the fractional inhibitory concentration index (FICI) for each drug pair. The fractional inhibitory concentration (FIC) for each combination was calculated as follows: FIC of **16** (or **17**) = MIC of 16 (or 17) in combination/MIC of 16 (or 17) alone; FIC of antibiotics = MIC of each antibiotic in combination/MIC of each antibiotic alone. FICI is the summation of FIC values for each drug. FICI results for each combination were interpreted as follows: ≤0.5, synergistic; >0.5 to ≤1.0, additive; >1.0 to ≤2.0, indifferent; and >2.0, antagonistic effects [41,42]. Similarly, the assay was performed for *C. albicans*, following the same procedure, but using the appropriate broth, antibiotic, and yeast dilution. The final concentration ranged from 0.03 to 32 μg/mL (0.03, 0.06, 0.12, 0.25, 0.5, 1, 2, 4, 8, 16, 32) for voriconazole and from 0.5 to 32 μg/mL (0.5, 1, 2, 4, 8, 16, 32) for (**16**) or (**17**).

4.7. ZebrafishsEmbryo Acute Toxicity

4.7.1. Ethics Statement

In vivo experiments have been performed at the facility for aquatic animal models at the Institute of Biomolecular Chemistry (ICB) of the National Research Council of Italy (CNR), approved by the Italian Ministry of Health (permission n. 20/2016-UT), according to Italian and European guidelines on research and to the guiding principles provided by the ICB body in charge of animal welfare (Organismo Preposto per il Benessere Animale—OPBA). Accordingly, treatments were carried out on larvae below 120 hpf, which are classified as non-protected under the EU Directive 2010/63/EU and are thus considered a valid alternative model to animal research [43].

4.7.2. Zebrafish fertilization and embryos collection

Adult fish were mantained at 28 °C in a ZebTec Active Blue–Stand Alone systems (Tecniplast, Varese, Italy) ZebTEC Active Blue Stand Alone (Tecniplast). Breeding was performed in a special spawning device, the 16-Liter Z-Park tank (Tecniplast, Varese, Italy). Collected embryos were maintained at 26 °C in a dark incubator in standard dilution water (294.0 mg/L $CaCl_2 \times 2H_2O$, 123.3 mg/L $MgSO_4 \times 7H_2O$, 64.7 mg/L $NaHCO_3$ and 5.7 mg/L KCl) [44]. Before treatments, embryos were checked under a light stereomicroscope for general health conditions and to assure they were at the same developmental stage [45].

4.7.3. Embryo treatments

Compounds **16** and **17** were dissolved in DMSO (99.9 %, Sigma-Aldrich) and then diluted in standard dilution water to obtain concentrations of 0.7, 2, 4, 8, 16, and 32 μg/mL with a 0.1 % as maximum concentration of DMSO. Within 4 hpf, embryos were transferred to 24-well plates (1 embryo per well) that were pre-incubated with the test solutions for 24 h. Each concentration was assayed on 20 embryos. Further two groups embryos (N = 20 per group) were exposed to 0.1 % DMSO (vehicle group), and to standard dilution water (control group). During the experiments, embryos were observed at 24, 48, 72 and 96 hpf under light stereomicroscope to follow their general health conditions and vitality. Toxicity was expressed as the concentration that is lethal to 50 % of zebrafish embryos (LC_{50}) calculated by probit analysis using R software (version 4.2.3) with the MASS package.

4.8. Statistical analysis

Each antimicrobial assay was repeated at least three times. Media and standard deviations are reported in figures.

CRediT authorship contribution statement

Marina Grinco: Data curation, Investigation, Methodology. **Olga Morarescu:** Data curation, Investigation, Methodology. **Francesca Lembo:** Data curation, Supervision, Validation. **Nicon Ungur:** Data curation, Validation. **Luigia Turco:** Investigation, Methodology. **Lorena Coretti:** Investigation, Methodology. **Marianna Carbone:** Investigation, Methodology. **Carmela Celentano:** Data curation, Investigation, Methodology. **Maria Letizia Ciavatta:** Investigation, Methodology, Writing – review & editing. **Ernesto Mollo:** Investigation, Methodology, Writing – original draft. **Veaceslav Kulcitki:** Conceptualization, Data curation, Validation, Writing – original draft. **Elisabetta Buommino:** Conceptualization, Data curation, Investigation, Writing – original draft.

Declaration of Competing Interest

The authors declare that they have no known competing financial interests or personal relationships that could have appeared to influence the work reported in this paper.

Data availability

No data was used for the research described in the article.

Acknowledgements

This research was funded by CNR (Italy)/ASM (Moldova) Joint Bilateral Program (grant number 18.80013.16.02.02/it) and the National Agency for Research and Development (ANCD) of the Republic of Moldova (grant number 20.80009.8007.03).

Appendix A. Supplementary data

Supplementary data to this article can be found online at https://doi.org/10.1016/j.ejmech.2023.115981.

References

[1] V.T. Anju, S. Busi, M. Imchen, R. Kumavath, M.S. Mohan, S.A. Salim, P. Subhaswaraj, M. Dyavaiah, Polymicrobial infections and biofilms: clinical significance and eradication strategies, Antibiotics 11 (2022) 1731, https://doi.org/10.3390/antibiotics11121731.

[2] H. Koo, R.N. Allan, R.P. Howlin, P. Stoodley, L. Hall-Stoodley, Targeting microbial biofilms: current and prospective therapeutic strategies, Nat. Rev. Microbiol. 15 (2017) 740–755, https://doi.org/10.1038/nrmicro.2017.99.

[3] R. Kean, R. Rajendran, J. Haggarty, E.M. Townsend, B. Short, K.E. Burgess, S. Lang, O. Millington, W.G. Mackay, C. Williams, G. Ramage, *Candida albicans* mycofilms support *Staphylococcus aureus* colonization and enhances miconazole resistance in dual-species interactions, Front. Microbiol. 8 (2017) 258, https://doi.org/10.3389/fmicb.2017.00258.

[4] Z. Zhao, J. Song, C. Yang, L. Yang, J. Chen, X. Li, Y. Wang, J. Feng, Prevalence of fungal and bacterial co-infection in pulmonary fungal infections: a metagenomic next generation sequencing-based study, Front. Cell. Infect. Microbiol. 11 (2021), 749905, https://doi.org/10.3389/fcimb.2021.749905.

[5] L.-A.J. Ghuneim, R. Raghuvanshi, K.A. Neugebauer, D.V. Guzior, M.H. Christian, B. Schena, J.M. Feiner, A. Castillo-Bahena, J. Mielke, M. McClelland, D. Conrad, I. Klapper, T. Zhang, R.A. Quinn, Complex and unexpected outcomes of antibiotic therapy against a polymicrobial infection, ISME J. 16 (2022) 2065–2075, https://doi.org/10.1038/s41396-022-01252-5.

[6] S.-H. Kim, D. Semenya, D. Castagnolo, Antimicrobial drugs bearing guanidine moieties: a review, Eur. J. Med. Chem. 216 (2021), 113293, https://doi.org/10.1016/j.ejmech.2021.113293.

[7] A. Dey, M. Yadav, D. Kumar, A.K. Dey, S. Samal, S. Tanwar, D. Sarkar, S. K. Pramanik, S. Chaudhuri, A. Das, A combination therapy strategy for treating antibiotic resistant biofilm infection using a guanidinium derivative and nanoparticulate Ag(0) derived hybrid gel conjugate, Chem. Sci. 13 (2022) 10103–10118, https://doi.org/10.1039/D2SC02980D.

[8] J. Li, X. Zhang, N. Han, P. Wan, F. Zhao, T. Xu, X. Peng, W. Xiong, Z. Zeng, Mechanism of action of isopropoxy benzene guanidine against multidrug-resistant pathogens, Microbiol. Spectr. 11 (1) (2023), e03469-22, https://doi.org/10.1128/spectrum.03469-22.

[9] O.V. Moshynets, T.P. Baranovskyi, O.S. Iungin, N.P. Kysil, L.O. Metelytsia, I. Pokholenko, V.V. Potochilova, G. Potters, K.L. Rudnieva, S.Y. Rymar, I. V. Semenyuta, A.J. Spiers, O.P. Tarasyuk, S.P. Rogalsky, eDNA inactivation and biofilm inhibition by the polymericbiocide polyhexamethylene guanidine hydrochloride (PHMG-Cl), Int. J. Mol. Sci. 23 (2022) 731, https://doi.org/10.3390/ijms23020731.

[10] R.G. Berlinck, D.I. Bernardi, T. Fill, A.A. Fernandes, I.D. Jurberg, The chemistry and biology of guanidine secondary metabolites, Nat. Prod. Rep. 38 (3) (2021) 586–667, https://doi.org/10.1039/D0NP00051E.

[11] A. Coqueiro, L.O. Regasini, P. Stapleton, V. da Silva Bolzani, S. Gibbons, *In vitro* antibacterial activity of prenylated guanidine alkaloids from *pterogyne nitens* and synthetic analogues, J. Nat. Prod. 77 (2014) 1972–1975, https://doi.org/10.1021/np500281c.

[12] K. Peng, T. Zou, W. Ding, R. Wang, J. Guo, J.J. Round, J. Hu, Development of contact-killing non-leaching antimicrobial guanidyl-functionalized polymers via click chemistry, RSC Adv. 7 (40) (2017) 24903–24913, https://doi.org/10.1039/C7RA02706K.

[13] C. Pasero, I. D'Agostino, F. De Luca, C. Zamperini, D. Deodato, G.I. Truglio, M. Botta, Alkyl-guanidine compounds as potent broad-spectrum antibacterial agents: chemical library extension and biological characterization, J. Med. Chem. 61 (20) (2018) 9162–9176, https://doi.org/10.1021/acs.jmedchem.8b00619.

[14] K. Pyta, A. Janas, M. Szukowska, P. Pecyna, M. Jaworska, M. Gajecka, P. Przybylski, Synthesis, docking and antibacterial studies of more potent amine and hydrazone rifamycin congeners than rifampicin, Eur. J. Med. Chem. 167 (2019) 96–104, https://doi.org/10.1016/j.ejmech.2019.02.009.

[15] A. Putz, S. Kehraus, G. Díaz-Agras, H. Wägele, G.M. König, Dotofide, a guanidine-interrupted terpenoid from the marine slug *Doto pinnatifida* (Gastropoda, Nudibranchia), Eur. J. Org Chem. (2011) 3733–3737, https://doi.org/10.1002/ejoc.201100347.

[16] S. Serra, A.A. Cominetti, V. Lissoni, Use of (S)- trans -γ-monocyclofarnesol as a useful chiral building block for the stereoselective synthesis of diterpenic natural products, Nat. Prod. Commun. 9 (2014), https://doi.org/10.1177/1934578X1400900312, 1934578X1400900.

[17] M. Carbone, M.L. Ciavatta, V. Mathieu, A. Ingels, R. Kiss, P. Pascale, E. Mollo, N. Ungur, Y.-W. Guo, M. Gavagnin, Marine terpenoid diacylguanidines: structure, synthesis, and biological evaluation of naturally occurring actinofide and synthetic analogues, J. Nat. Prod. 80 (2017) 1339–1346, https://doi.org/10.1021/acs.jnatprod.6b00941.

[18] P.-H. Hsu, D.-C. Chiu, K.-L. Wu, P.-S. Lee, J.-T. Jan, Y.-S.E. Cheng, K.-C. Tsai, T.-J. Cheng, J.-M. Fang, Acylguanidine derivatives of zanamivir and oseltamivir: potential orally available prodrugs against influenza viruses, Eur. J. Med. Chem. 154 (2018) 314–323, https://doi.org/10.1016/j.ejmech.2018.05.030.

[19] J.-J. Shie, J.-M. Fang, Development of effective anti-influenza drugs: congeners and conjugates – a review, J. Biomed. Sci. 26 (2019) 84, https://doi.org/10.1186/s12929-019-0567-0.

[20] G. Duca, A. Aricu, K. Kuchkova, E. Secara, A. Barba, I. Dragalin, N. Ungur, G. Spengler, Synthesis, structural elucidation and biological evaluations of new guanidine-containing terpenoids as anticancer agents, Nat. Prod. Res. 33 (2019) 3052–3056, https://doi.org/10.1080/14786419.2018.1516658.

[21] D.M.P. De Oliveira, B.M. Forde, T.J. Kidd, P.N.A. Harris, M.A. Schembri, S. A. Beatson, D.L. Paterson, M.J. Walker, Antimicrobial resistance in ESKAPE pathogens, Clin. Microbiol. Rev. 33 (3) (2020) 10–1128, https://doi.org/10.1128/CMR.00181-19.

[22] S.-K. Hua, J. Wang, X.-B. Chen, Z.-Y. Xu, B.-B. Zeng, Scalable synthesis of methyl ent-isocopalate and its derivatives, Tetrahedron 67 (2011) 1142–1144, https://doi.org/10.1016/j.tet.2010.12.008.

[23] P.F. Vlad, N.D. Ungur, N. Van Tuen, Superacidic cyclization of higher terpenoid acids and their esters, Russ. Chem. Bull. 44 (1995) 2404–2411, https://doi.org/10.1007/BF00713614.

[24] P.F. Vlad, A.N. Aryku, A.G. Chokyrlan, Synthesis of (+)-drim-9(11)-en-8 -ol from sclareol, Russ. Chem. Bull. 53 (2004) 443–446, https://doi.org/10.1023/B:RUCB.0000030822.72251.ea.

[25] A.G. González, B.M. Fraga, M.G. Hernández, F. Larruga, J.G. Luis, Four new labdane diterpene oxides from *Sideritis gomerae*, Phytochemistry 14 (1975) 2655–2656, https://doi.org/10.1016/0031-9422(75)85244-7.

[26] C. Fernández, B.M. Fraga, M.G. Hernández, Diterpenes from *Sideritis nutans*, Phytochemistry 25 (1986) 2825–2827, https://doi.org/10.1016/S0031-9422(00)83750-4.

[27] O. Morarescu, M. Traistari, A. Barba, G. Duca, N. Ungur, V. Kulciţki, One-step selective synthesis of 13-*epi*-manoyl oxide, Chem. J. Mold. 16 (2021) 99–104, https://doi.org/10.19261/cjm.2021.820.

[28] A. Dondoni, A. Marra, C-glycofuranosides via tandem Wittig-Michael sequence using a thiazole-armed phosphorane. A route to C-furanosyl α-hydroxy propanals and propionic acids, Tetrahedron Lett. 34 (1993) 7327–7330, https://doi.org/10.1016/S0040-4039(00)79321-X.

[29] C.F. Nising, S. Bräse, Recent developments in the field of oxa-Michael reactions, Chem. Soc. Rev. 41 (2012) 988–999, https://doi.org/10.1039/C1CS15167C.

[30] T. Ahmad, N. Ullah, The oxa-Michael reaction in the synthesis of 5- and 6-membered oxygen-containing heterocycles, Org. Chem. Front. 8 (2021) 1329–1344, https://doi.org/10.1039/D0QO01312A.

[31] A.K. Mailyan, K.Y. Joanna, J.L. Chen, B.T. Reid, A. Zakarian, Stereoselective synthesis of cyclic guanidines by directed diamination of unactivated alkenes, Org. Lett. 18 (2016) 5532–5535, https://doi.org/10.1021/acs.orglett.6b02778.

[32] Version 12.0, The European Committee on Antimicrobial Susceptibility Testing, Breakpoint Tables for Interpretation of MICs and Zone Diameters, 2022, http://www.eucast.org.

[33] Clinical and laboratory standards institute (CLSI), Performance Standards for Antifungal Susceptibility Testing of Yeasts, third ed., CLSI supplement M27M44S, 2022.

[34] M. Laws, A. Shaaban, K.M. Rahman, Antibiotic resistance breakers: current approaches and future directions, FEMS (Fed. Eur. Microbiol. Soc.) Microbiol. Rev. 43 (5) (2019) 490–516, https://doi.org/10.1093/femsre/fuz014.

[35] N.E. White, M. Kilpatrick, Association of NH compounds. I. In benzene, J. Phys. Chem. 59 (10) (1955) 1044–1053, https://doi.org/10.1021/j150532a013.

[36] A.T. Banyikwa, A. Goos, D.J. Kiemle, M.A. Foulkes, M.S. Braiman, Experimental and computational modeling of H-bonded arginine–tyrosine groupings in aprotic environments, ACS Omega 2 (9) (2017) 5641–5659, https://doi.org/10.1021/acsomega.7b00282.

[37] P. Li, Y. Wu, Y. Wang, J. Qiu, Y. Li, Soil behaviour of the veterinary drugs lincomycin, monensin, and roxarsone and their toxicity on environmental organisms, Molecules 24 (2019) 4465, https://doi.org/10.3390/molecules24244465.

[38] E. Praskova, E. Voslarova, Z. Siroka, L. Plhalova, S. Macova, P. Marsalek, V. Pistekova, Z. Svobodova, Assessment of diclofenac LC50 reference values in juvenile and embryonic stages of the zebrafish (*Danio rerio*), Pol. J. Vet. Sci. 14 (2011) 545–549, https://doi.org/10.2478/v10181-011-0081-0.

[39] J.M. Castro, S. Salido, J. Altarejos, M. Nogueras, A. Sánchez, Synthesis of Ambrox® from labdanolic acid, Tetrahedron 58 (2002) 5941–5949, https://doi.org/10.1016/S0040-4020(02)00571-9.

[40] E. Buommino, S. De Marino, M. Sciarretta, M. Piccolo, C. Festa, M.V. D'Auria, Synergism of a novel 1,2,4-oxadiazole-containing derivative with oxacillin against methicillin-resistant *Staphylococcus aureus*, Antibiotics 10 (2021) 1258, https://doi.org/10.3390/antibiotics10101258.

[41] F.C. Odds, Synergy, antagonism, and what the chequerboard puts between them, J. Antimicrob. Chemother. 52 (2003) 1, https://doi.org/10.1093/jac/dkg301.

[42] S.K. Pillai, R.C. Moellering, G.M. Eliopoulos, Antimicrobial combinations, in: V. Lorian (Ed.), Antibiotics in Laboratory Medicine, fifth ed., the Lippincott Williams & Wilkins Co., Philadelphia, 2005, pp. 365–440.

[43] R. Geisler, A. Köhler, T. Dickmeis, U. Strähle, Archiving of zebrafish lines can reduce animal experiments in biomedical research, EMBO Rep. 18 (2017) 1–2, https://doi.org/10.15252/embr.201643561.

[44] F. Busquet, R. Strecker, J.M. Rawlings, S.E. Belanger, T. Braunbeck, G.J. Carr, P. Cenijn, P. Fochtman, A. Gourmelon, N. Hübler, A. Kleensang, M. Knöbel, C. Kussatz, J. Legler, A. Lillicrap, F. Martínez-Jerónimo, C. Polleichtner, H. Rzodeczko, E. Salinas, K.E. Schneider, S. Scholz, E.-J. van den Brandhof, L.T. M. van der Ven, S. Walter-Rohde, S. Weigt, H. Witters, M. Halder, OECD validation study to assess intra- and inter-laboratory reproducibility of the zebrafish embryo toxicity test for acute aquatic toxicity testing, Regul. Toxicol. Pharmacol. 69 (2014) 496–511, https://doi.org/10.1016/j.yrtph.2014.05.018.

[45] C.B. Kimmel, W.W. Ballard, S.R. Kimmel, B. Ullmann, T.F. Schilling, Stages of embryonic development of the zebrafish, Dev. Dynam. 203 (1995) 253–310, https://doi.org/10.1002/aja.1002030302.